Multipartite entanglement from consecutive scatterings

Gonçalo M. Quinta[*] and Rui André[†]

Instituto de Telecomunicações, Lisbon, Portugal

We study how the successive scattering of spin-1/2 particles with a central spin-1/2 target particle can generate entanglement between the helicity degrees of freedom of all scattered particles, effectively producing a multipartite entangled state. We show that the bipartite entanglement between each pair of scattered particles, as quantified by the concurrence, is largest for reflected particles and decreases with the number of scatterings. We study the entanglement generation as a function of the scattered particles momenta, angular distribution, and mass ratios, and show that there is always a combination of optimal helicities and momentum, which generate the largest amount of bipartite entanglement.

I. INTRODUCTION

The development rate of quantum technologies is inherently dependent on the ability to generate and manipulate entanglement in quantum states. Despite the many decades necessary to manifest entanglement in the laboratory, it is now considered a physical resource able to be, among other things, manipulated [1–4] and distributed [5–7]. The vast majority of quantum information applications, such as dense coding, quantum teleportation, quantum key distribution [8], error correcting codes [9], or quantum computation [10,11] are in fact, in one way or another, a particular way to exploit the properties of quantum entanglement.

To generate entanglement, one needs to make at least two systems interact in such a way that their quantum degrees of interest are not measured after the interaction. The most natural setup in which this occurs is during particle collisions. In fact, any quantum mechanical interaction is most fundamentally described by quantum field theory (QFT), so it is expected that the generation of entanglement is rooted in the interactions of elementary particles, scatterings being the most common ones. Research on the role of entanglement generation has gained particular traction in recent years in several fields of high-energy physics, such as neutrino oscillations [12–16], quantum electrodynamics (QED) [17–19], and quantum chromodynamics [20]. However, particle scatterings have gained a particular emphasis due to their conceptual simplicity and richness. The typical physical setup consists in considering the helicity quantum degrees of freedom of two initially separated particles, which become entangled after the collision. Using Feynman diagrams, it is straightforward to investigate all manners of entanglement generation for different types of interaction, a topic that has attracted some attention in recent years [21–27]. Connections between entanglement minimization and the emergence of QCD symmetries have

also recently been suggested [28–32]. The generation of entanglement specifically through particle scatterings has been studied in QED in Ref. [17], where maximal entanglement between helicity degrees of freedom was shown not only to be present in most possible scatterings but also possibly related to gauge symmetry of QED. A more in-depth treatment of entanglement generation in QED scatterings was also performed in Ref. [18]. In a context of more than two particles, it was shown recently [19] that the cross-sectional information between two-particle collisions can be encoded in a third spectator particle, as long as it is initially entangled with one of the scattered particles. Overall, two-particle scattering scenarios have been reasonably explored but scatterings of multiple particles have not been addressed to date.

Particle scatterings typically happen in a small time window, which makes it very unlikely that more than two particles actually collide at the same time in such a way that multiple particles need to be considered in a single Feynman diagram. Nevertheless, multiple consecutive two-particle scatterings can occur before any of the final states are collapsed. This leads to a picture where particles in entangled states coming from past scatterings can collide with new separable particles, resulting in increasingly larger multiparticle entangled states.

In this work, we explore this simple scenario and analyze its usefulness as a method to create multipartite entangled states. In particular, we consider a spin-1/2 target particle initially at rest and subject it to consecutive collisions with lighter projectile particles coming from an external source. Although we do not develop on the experimental side, this work provides a conceptual method that indeed generates multipartite states from collisions and shows what entanglement properties one can expect from such states.

II. ENTANGLEMENT IN PARTICLE SCATTERINGS

We begin by specifying the nomenclature used throughout this work (following that of Ref. [33]) and show how entanglement is naturally present in the quantum degrees of freedom involved in particle scatterings, specifically for the fermionic

---

*goncalo.quinta@tecnico.ulisboa.pt
†rui.andre@tecnico.ulisboa.pt

case. Consider n particles with masses m_i at a certain time instant $t = t_i$, labeled by their three-vector momenta $\mathbf{p}_i$ and basis indexes h_i, where henceforth we will use bold notation for three-vectors. The h_i can be related to spin or helicity, for example. For simplicity, we will restrict this work to the case of equal number of initial and final particles as well as the conservation of the number of each particle species present in the reaction. We assume that at t_i they are sufficiently far away such that together they are in an eigenstate of the free Hamiltonian, written in the form

$$|\psi(t_i)\rangle = |\mathbf{p}_1, h_1; \ldots; \mathbf{p}_n, h_n\rangle. \quad (1)$$

After a certain period of time they interact and scatter, and at a further enough time instant we consider them again to be in an eigenstate of the free theory. This evolution is encoded in the scattering matrix, given by

$$\hat{U} = T\left\{\exp\left(-i \int_{-\infty}^{+\infty} \hat{V}(t')dt'\right)\right\}, \quad (2)$$

where T is the time-ordering operator and $\hat{V}(t')$ is the potential part of the Hamiltonian in the interaction picture and a hat notation will be adopted for operators. The scattered state is thus of the form

$$|\psi(t_f)\rangle = \hat{U}|\psi(t_i)\rangle = (1 + i\hat{T})|\psi(t_i)\rangle, \quad (3)$$

where we used the standard decomposition $\hat{U} = 1 + i\hat{T}$. We will use the standard nomenclature

$$\langle\mathbf{q}_1, r_1; \ldots; \mathbf{q}_n, r_n| i\hat{T}|\mathbf{p}_1, h_1; \ldots; \mathbf{p}_n, h_n\rangle$$
$$= (2\pi)^4 \delta^{(4)}\left(\sum q_i - \sum p_i\right)$$
$$\times i\mathcal{M}(\mathbf{q}_1, r_1; \ldots; \mathbf{q}_n, r_n|\mathbf{p}_1, h_1; \ldots; \mathbf{p}_n, h_n) \quad (4)$$

for the nontrivial piece of the scattering amplitude from the initial state $|\psi(t_i)\rangle$ to an n-particle state with momenta $\mathbf{q}_i$ and basis index r_i, where the Dirac δ ensures momentum conservation. The crucial point of Eq. (3) is that, so long as the final dynamical quantities are not measured, the final state will be in a superposition of all possible outgoing states. This can be seen by applying the n-particle identity operator $\hat{I}_n$ from the left in Eq. (3), where

$$\hat{I}_n = \int \frac{d^3\mathbf{q}_1}{(2\pi)^3 2E_{\mathbf{q}_1}} \cdots \frac{d^3\mathbf{q}_n}{(2\pi)^3 2E_{\mathbf{q}_n}}$$
$$\times \sum_{r_1, \ldots, r_n} |\mathbf{q}_1, r_1; \ldots; \mathbf{q}_n, r_n\rangle \langle\mathbf{q}_1, r_1; \ldots; \mathbf{q}_n, r_n|, \quad (5)$$

where $d^3\mathbf{q} \equiv dq_x dq_y dq_z$ is the spatial volume element and $E_{\mathbf{p}_i} = \sqrt{|\mathbf{p}_i|^2 + m_i^2}$ are the particles' energies. This leads to the following form for the final state:

$$|\psi(t_f)\rangle = |\psi(t_i)\rangle + i(2\pi)^4 \int \frac{d^3\mathbf{q}_1}{(2\pi)^3 2E_{\mathbf{q}_1}} \cdots \frac{d^3\mathbf{q}_n}{(2\pi)^3 2E_{\mathbf{q}_n}} \delta^{(4)}$$
$$\times \left(\sum q_i - \sum p_i\right) \sum_{r_1, \ldots, r_n} \mathcal{M}(\mathbf{q}_1, r_1; \ldots; \mathbf{q}_n,$$
$$r_n|\mathbf{p}_1, h_1; \ldots; \mathbf{p}_n, h_n)|\mathbf{q}_1, r_1; \ldots; \mathbf{q}_n, r_n\rangle, \quad (6)$$

which clearly shows that the final state is a superposition of all possible $|\mathbf{q}_1, r_1; \ldots; \mathbf{q}_n, r_n\rangle$. Such a superposition will

in general be impossible to decompose as a tensor product, indicating that the final state will be entangled in general.

Finally, it is important to note that the initial state $|\psi(t_i)\rangle$ can also be entangled from the very beginning, even if the particles are very far away from each other. Indeed, such a group of particles might have originated from a different scattering and as a consequence became entangled. This is also fully consistent with the free theory eigenstate assumption. To see this, consider the general free theory Hamiltonian written in second quantized form

$$\hat{H}_0 = \int \frac{d^3\mathbf{p}}{(2\pi)^3} \sum_h E_{\mathbf{p}} \hat{a}_{\mathbf{p}}^{h\dagger} \hat{a}_{\mathbf{p}}^h, \quad (7)$$

where $\hat{a}_{\mathbf{p}}^h$ is the annihilation operator, i.e., the anticommuting operator, which annihilates the free theory vacuum $|0\rangle$ and obeys the relation

$$\{\hat{a}_{\mathbf{p}}^h, \hat{a}_{\mathbf{p}'}^{h'\dagger}\} = (2\pi)^3 \delta_{hh'} \delta(\mathbf{p} - \mathbf{p}'). \quad (8)$$

The initial state can then be written as

$$|\mathbf{p}_1, h_1; \ldots; \mathbf{p}_n, h_n\rangle = (2^n E_{\mathbf{p}_1} \cdots E_{\mathbf{p}_n}) \hat{a}_{\mathbf{p}_1}^{h_1\dagger} \ldots \hat{a}_{\mathbf{p}_n}^{h_n\dagger}|0\rangle. \quad (9)$$

Focusing on the helicity quantum degrees of freedom, which are what we will be concerned with in this work, if we consider a general linear combination of the form

$$|\tilde{\psi}\rangle = \sum_{h_1 \ldots h_n} c_{h_1 \ldots h_n} |\mathbf{p}_1, h_1; \ldots; \mathbf{p}_n, h_n\rangle, \quad (10)$$

one can straightforwardly conclude from Eq. (8) that

$$\hat{H}_0|\tilde{\psi}\rangle = \left(\sum_i E_{\mathbf{p}_i}\right)|\tilde{\psi}\rangle \quad (11)$$

and so one proves that $|\tilde{\psi}\rangle$ is also an eigenstate of the free theory. Since $|\tilde{\psi}\rangle$ represents a general form of an entangled state, one thus concludes that entangled states are also eigenstates of the free theory.

III. A SINGLE SCATTERING

We will focus first on the entanglement generated from a single scattering, taking the limit where both projectile and target particles are pointlike with no internal structure. The setup consists of a target particle of rest-mass M with four-momentum $p_1 = (M, 0, 0, 0)$, and a projectile particle of rest-mass m aligned with the z axis with four-momentum $p_2 = (\sqrt{m^2 + p^2}, 0, 0, p)$ fired at the target particle. Ideally, the target particle is heavy enough (compared to the projectile one) for the recoil to be considered negligible, in order to experimentally facilitate multiple collisions with the same heavy particle. From the theoretical perspective of this work, we consider that each projectile particle always hits the target particle. The direction of the outgoing projectile particles is determined by the angles θ and ϕ, corresponding to the azimuthal and polar angles, respectively, where from polar symmetry we can fix $\phi = 0$ in the first collision. The quantum degrees of freedom whose entanglement we would like to study are the helicities of both particles, which start out in a separable state. Denoting the initial and final helicities of the projectile and target particles as h_1, h_2 and h_3, h_4, respectively,
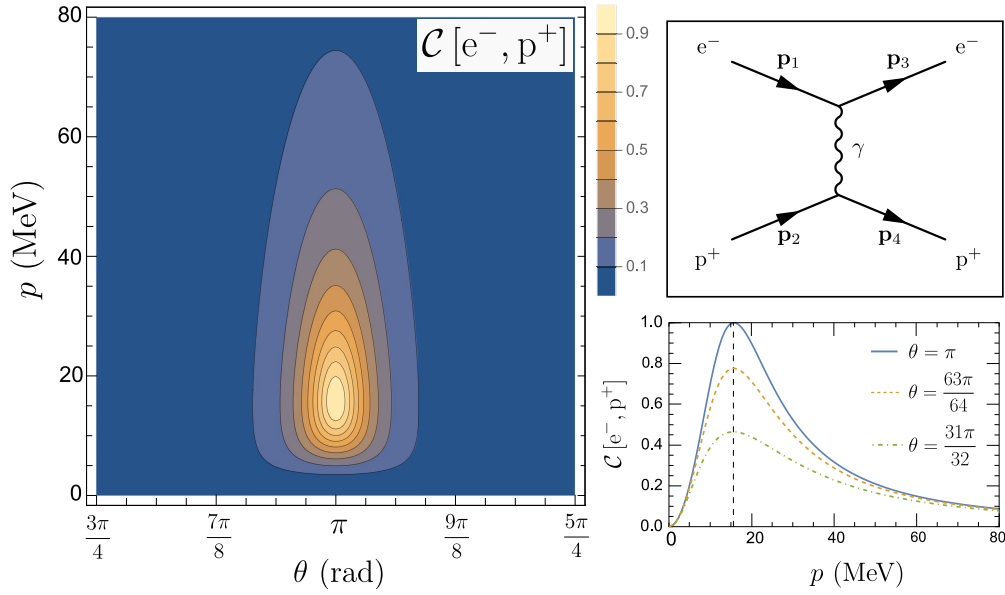
FIG. 1. Top right: The Feynman diagram of the interaction. Left half and bottom right: Concurrence generated from scattering an electron off a proton at rest in the laboratory frame. Choosing as initial state a polarized state where both particles have opposing helicities yields maximal entanglement, i.e., $\mathcal{C} = 1$, for $\theta = \pi$ and $p \approx 15.1$ MeV. For a fixed momentum p, the outgoing electron has a single degree of freedom in θ such that $\mathbf{p}_4 = \mathbf{p}_4(\theta)$ (cf. Appendix B). The domain $\theta \in [3\pi/4, 5\pi/4]$ was chosen to facilitate the visualization of the region with appreciable entanglement generation.

one can apply the unitary evolution operator $\hat{U}_{1,2}$ defined as $\hat{U}$ from Eq. (2) acting on two particles and contract the result with $\langle \mathbf{p}_3, h_3; \mathbf{p}_4, h_4 |$. This leads to the transition probability for the case where the scattering occurs, given by (see Appendix A)

$$\langle \mathbf{p}_3, h_3; \mathbf{p}_4, h_4 | \hat{U}_{1,2} | \mathbf{p}_1, h_1; \mathbf{p}_2, h_2 \rangle$$
$$= \mathcal{N}_2 \, \mathcal{M}(\mathbf{p}_1 + \mathbf{p}_2 - \mathbf{p}_4, h_3; \mathbf{p}_4, h_4 | \mathbf{p}_1, h_1; \mathbf{p}_2, h_2), \quad (12)$$

where three-momentum conservation is evident and the normalization factor

$$\mathcal{N}_2 = i(2\pi)^4 \delta\big(E_{\mathbf{p}_3} + E_{\mathbf{p}_4} - E_{\mathbf{p}_1} - E_{\mathbf{p}_2}\big) \quad (13)$$

ensures conservation of energy. Focusing on the helicity degrees of freedom, one finds that the final state is of the form

$$|\psi_f\rangle = \sum_{h_3, h_4} \mathcal{M}(h_3, h_4 | h_1, h_2) |h_3, h_4\rangle, \quad (14)$$

where we omit the momentum notation and superfluous constant factors. Momentum and energy conservation are always implicit, despite the omission of momentum vector variables. The state $|\psi_f\rangle$ is a two-qubit state, where we consider the index 0 and 1 to be associated to the helicities $+1$ and -1, respectively. The entanglement between the helicity (qubit) degrees of freedom can be quantified by the concurrence [34], denoted here by $\mathcal{C}$. This quantity can be expressed as

$$\mathcal{C}(\rho) = \max(0, \lambda_1 - \lambda_2 - \lambda_3 - \lambda_4), \quad (15)$$

where $\lambda_1, \ldots, \lambda_4$ are the eigenvalues, in decreasing order, of the Hermitian matrix

$$R = \sqrt{\sqrt{\rho} \tilde{\rho} \sqrt{\rho}} \quad (16)$$

with

$$\tilde{\rho} = (\sigma_y \otimes \sigma_y) \rho^* (\sigma_y \otimes \sigma_y), \quad (17)$$

where σ_y are the Pauli matrices in the y direction and ρ is the density matrix of the system. For simplicity, we will denote the concurrence between particles A and B as $\mathcal{C}[A, B]$. Although any superposition of helicities can be considered as an initial state, it is more convenient to start with a separable state in order to to investigate how much entanglement was generated. The only helicity state that can yield maximal entanglement, i.e., $\mathcal{C} = 1$, is that of opposite helicities, such as $|01\rangle$. Consequently, it will be the case of focus in this section. Additionally, we will focus on the entanglement being generated on the vicinity of $\theta = \pi$, as it has already been seen [18] that this is the most prolific case for entanglement generation in t-channel QED scatterings.

Figure 1 illustrates the entanglement generation for different initial momentum p and scattering angle θ for an initial state of the form $|01\rangle$, for the particular case of an electron scattering off a proton. One finds that, for most angles and momenta, the scattering does not generate any entanglement.

However, it is interesting to note that for situations where the electron reflects off the proton, i.e., $\theta \approx \pi$, the particles become entangled, and can even reach maximal entanglement for $\theta = \pi$ and $p = \sqrt{\frac{Mm}{2}}(1 - \sqrt{\frac{m/M}{2}} + \mathcal{O}(m/M)) \approx 15.1$ MeV, an energy which is not high enough to relevantly probe the proton's internal structure, so we ignore the contribution of the proton's form factor to the scattering amplitudes. The existence of an optimal momentum is actually expected on intuitive grounds: for very small or very large momenta, the projected particle barely interacts with the target particle, leading to small entanglement, so there must be a middle ground
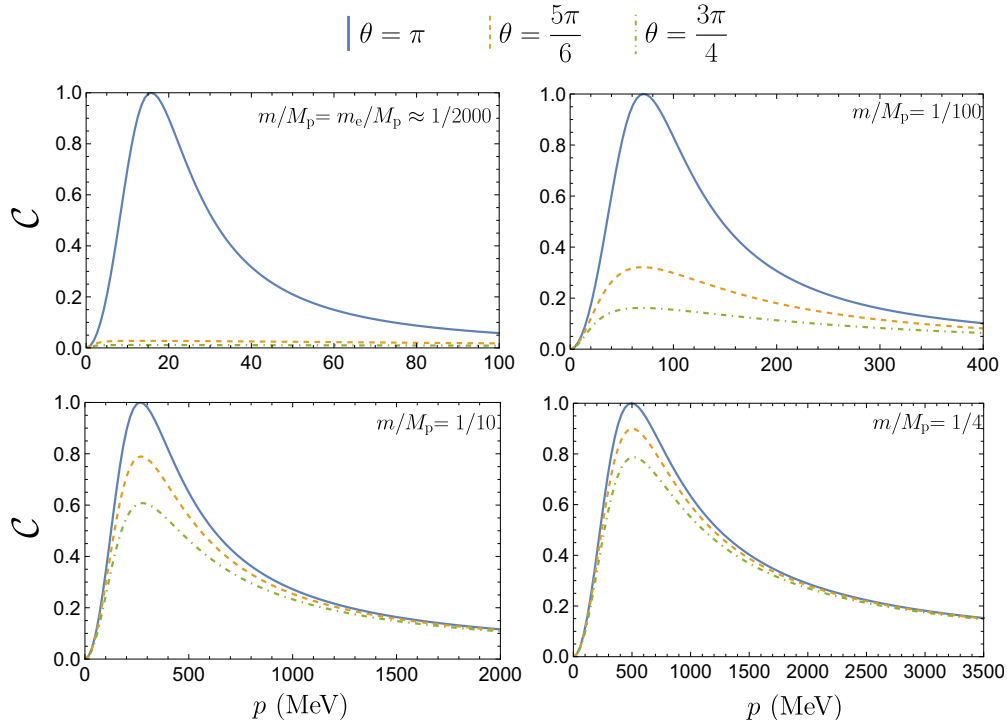
FIG. 2. Concurrence between the scattered particles qubit helicity degrees of freedom for the single scattering scenario. Each label is aligned with the corresponding plot line. The target particle is fixed as proton with mass $M = M_p$, while the smaller particle is considered for four different possible masses. In each of the four cases, the concurrence is plotted for a set of values of the scattering angle θ to illustrate how the entanglement is more easily generated for higher values of the mass ratio m/M_p. This, however, comes at the expense of requiring higher momenta for the accelerated particle to achieve maximum entanglement.

where the interaction is stronger, leading to the maximal possible generated entanglement. Nevertheless, the same process between particles with different mass ratios can accommodate a much larger θ variation. To see this, we can redo the concurrence plot of Fig. 1 for different projectile particle masses, as is done in Fig. 2. It is evident that it becomes possible generate entanglement for larger angular apertures as the projectile particle's mass approaches that of the target particle's. This will come at the cost of requiring a larger momentum for the projectile particle.

IV. CONSECUTIVE SCATTERINGS

We are now interested in the situation where, after the first two-particle scattering, one of the scattered particles interacts again with a third particle, without ever having its state collapsed. Assuming that enough time and space are given, the second scatter takes as initial state's particles, which are under the influence of the free Hamiltonian, thus one may consider again that the interaction is governed by the unitary operator of Eq. (3). We can now apply this operator two consecutive times: one for the scattering of the first projectile particle with the target particle and another for the scattering of the second projectile particle with the recoiled target particle. Finally, since we wish to study the entanglement generated in the qubit degrees of freedom associated to the helicities, we will focus on the helicity component of the final state. The result is the

following state (proof in Appendix A):

$$|\psi_h\rangle = \mathcal{N}_3 \sum_{h_4, h_5, h_6} d_{h_4 h_5 h_6}(\mathbf{p}_4, \mathbf{p}_5, \mathbf{p}_6)|h_4, h_5, h_6\rangle, \qquad (18)$$

where $\mathbf{p}_4$, $\mathbf{p}_5$, $\mathbf{p}_6$ and h_4, h_5, h_6 are the momenta and helicities of the target, first, and second projectile particles, respectively, and

$$d_{h_4 h_5 h_6}(\mathbf{p}_4, \mathbf{p}_5, \mathbf{p}_6)$$
$$= \sum_{r_1} \mathcal{M}(\mathbf{p}_4, h_4; \mathbf{p}_6, h_6 | \mathbf{p}_5 - \mathbf{p}_1 - \mathbf{p}_2, r_1; \mathbf{p}_3, h_3)$$
$$\times \mathcal{M}(\mathbf{p}_5 - \mathbf{p}_1 - \mathbf{p}_2, r_1; \mathbf{p}_5, h_5 | \mathbf{p}_1, h_1; \mathbf{p}_2, h_2) \quad (19)$$

are the components of the state, with

$$\mathcal{N}_3 = -\frac{(2\pi)^5}{2E_{\mathbf{p}_5-\mathbf{p}_1-\mathbf{p}_2}} \delta\big(E_{\mathbf{p}_5-\mathbf{p}_1-\mathbf{p}_2} + E_{\mathbf{p}_5} - E_{\mathbf{p}_1} - E_{\mathbf{p}_2}\big)$$
$$\times \delta\big(E_{\mathbf{p}_5-\mathbf{p}_1-\mathbf{p}_2} + E_{\mathbf{p}_3} - E_{\mathbf{p}_4} - E_{\mathbf{p}_6}\big)$$
$$\times \delta^{(3)}(\mathbf{p}_1 + \mathbf{p}_2 + \mathbf{p}_3 - \mathbf{p}_4 - \mathbf{p}_5 - \mathbf{p}_6) \quad (20)$$

being formally a constant, which enforces conservation of momentum and energy over the set of scatterings that occur by means of Dirac δ. It is worthwhile to note that while the two electrons are intrinsically indistinguishable, one can distinguish each of them by time of scattering, such that each qubit has an unambiguous association. For example, Alice retains the electron from the first interaction and Bob retains the second, such that they can now share a two-particle entangled
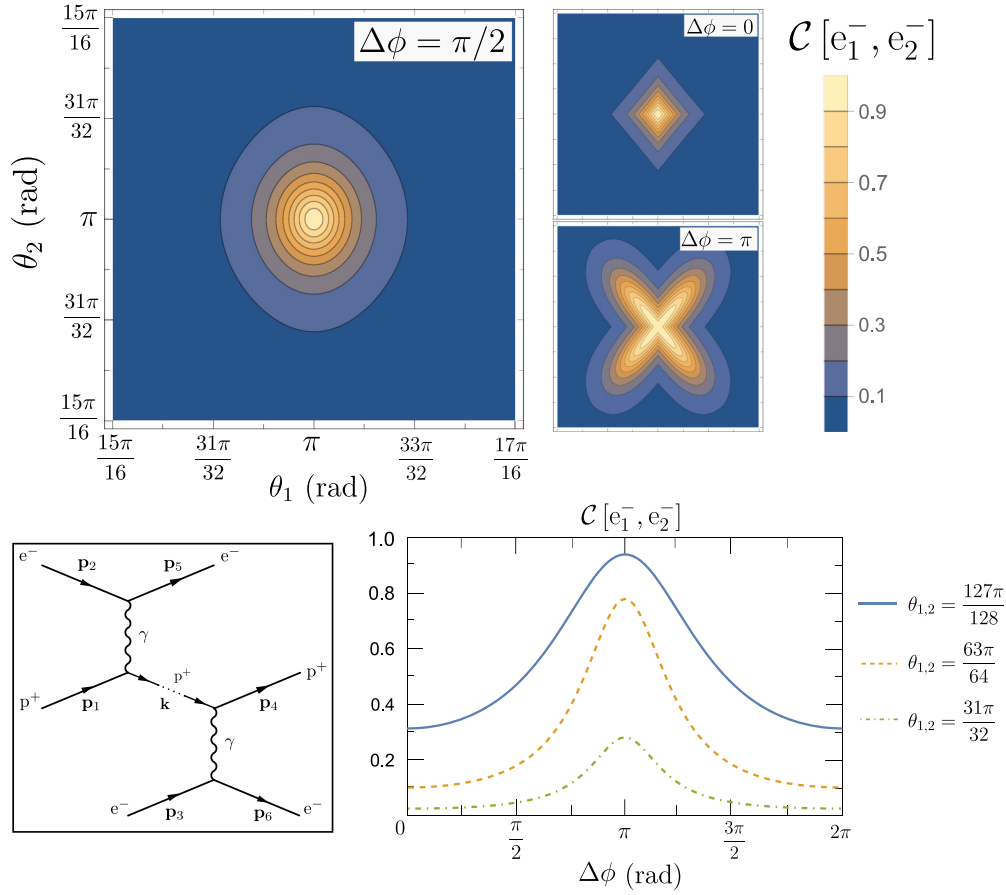
FIG. 3. Bottom left: Feynman diagrams for two consecutive scatterings between two electrons and a proton. The dashed line represents a scattered proton external line for both diagrams. Top half and bottom right: Concurrence generated from scattering two electrons with momenta $p \approx 47.16$ MeV off a proton at rest in the laboratory frame. Choosing for the initial state a polarized state where both electrons have a helicity orthogonal to the proton's starting helicity maximizes the entanglement generated. The relative positions in the cone are also relevant. For a fixed momentum p, the outgoing electrons have a total of three degrees of freedom θ_1, θ_2 and $\Delta\phi$, such that $\mathbf{p}_5 = \mathbf{p}_5(\theta_1)$ and $\mathbf{p}_6 = \mathbf{p}_6(\theta_2, \Delta\phi)$ (cf. Appendix B). Entanglement is maximized for $\theta_{1,2} = \pi$, $\Delta\phi = \pi$, and $p \approx 47.16$ MeV, but fails to reach maximal value between the two electrons. The domain is chosen as $[15\pi/16, 17\pi/16]$ for each polar angular variable to facilitate the visualization of the region with appreciable entanglement generation.

state. The particular setup of this work does not contain any indistinguishability effects, which would be naturally included in the scattering amplitudes $\mathcal{M}$ appearing within the unitary evolution operators acting on the initial state.

To study the entanglement of the system one first needs to construct the density matrix

$$\rho_{t,p,p} = \frac{|\psi_h\rangle \langle\psi_h|}{\text{Tr}[|\psi_h\rangle \langle\psi_h|]}, \tag{21}$$

whose normalization eliminates the cumbersome $\mathcal{N}_3$ factor. The amount of bipartite entanglement generated between the two projectile particles is obtained by using the reduced density matrix derived by tracing out the target particle qubit t, resulting in the density matrix (proof in Appendix A)

$$\rho_{p,p} = \text{Tr}_t[\rho_{t,p,p}]$$
$$= \sum_{h_5,h_6,r_5,r_6} \rho_{h_5 h_6 r_5 r_6} |h_5, h_6\rangle \langle r_5, r_6|, \tag{22}$$

where we have the reduced density matrix components

$$\rho_{h_5 h_6 r_5 r_6} = \frac{\sum_\sigma d_{\sigma h_5 h_6}(\mathbf{p}_4, \mathbf{p}_5, \mathbf{p}_6) d^*_{\sigma r_5 r_6}(\mathbf{p}_4, \mathbf{p}_5, \mathbf{p}_6)}{\sum_{h_4,h_5,h_6} |d_{h_4 h_5 h_6}(\mathbf{p}_4, \mathbf{p}_5, \mathbf{p}_6)|^2}. \tag{23}$$

To calculate the entanglement between the two projectiles' helicities we find the concurrence $\mathcal{C}[p, p]$ by using Eq. (15) for the reduced density matrix in Eq. (23).

We now wish to apply the precedent reasoning to the scenario where two projectiles originating from the same source, i.e., both described by the four-momentum $p_1 = (\sqrt{m^2 + p^2}, 0, 0, p)$, scatter at different instants off a target, which started at rest, as illustrated in the diagram in Fig. 3. It can be shown that only three degrees of freedom are associated to the two outgoing projectiles (cf. Appendix B): the polar angle θ_1 of the first scattered projectile, the polar angle θ_2 of the second scattered projectile, and the azimuth angle difference between the two, denoted by $\Delta\phi$. As reported in the previous section, entanglement is maximized for θ close to π, so it is expected that the two projectiles are more entangled close to this value as well. Figure 3 evidently displays this behavior, for a fixed momentum $p \approx 47.16$ MeV,
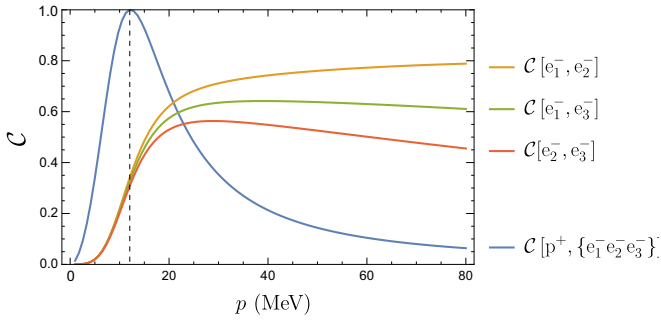
FIG. 4. Concurrence between subsystems resulting from three reflected collisions, for the maximal generation case of reflected particles. The proton can be maximally entangled with the subsystem of three electrons, which describes a qudit of 2^3 levels, at a relatively low energy of $p \approx 12.06$ MeV.

which maximizes the concurrence for the particular case of electrons being fired at a proton. It is interesting to note how the degree of freedom $\Delta\phi$ affects the concurrence in Fig. 3. If we consider a fixed value for both θ_1 and θ_2, we can interpret the two electrons as being reflected along the surface of a cone centered around the z axis, such that $\Delta\phi$ indicates how distant the two electrons lie on the cone. It is clear that the more distant apart the electrons are in the surface of the cone, the more entanglement is generated, reaching a maximum when they are on opposite sides of the cone with $\Delta\phi = \pi$.

The electron momentum maximizing the entanglement in this scenario is larger than the one required in the single scattering scenario of Fig. 1. This is due to the fact that the proton from the first scattering acquires a momentum of roughly $2p$ after the initial scatter, where θ_1 is close to π. Since the scattered proton is moving away from the second electron, the relative momentum between the two is thus smaller than in the first scattering so the electrons momentum needs to be larger to compensate for this difference, in order to achieve the optimal relative momentum derived in Sec. III.

To have an intuition of how the entanglement will be distributed with more scatterings, one can calculate the case of three scatterings. The latter calculations are straightforwardly generalizable from the derivations in Appendixes A and B. Although there is not a single measure to quantify the entanglement present in the resulting four-qubit state, one can calculate the entanglement between the relevant bipartitions, namely between all pairs of electrons and between the proton and all other electrons. This is represented in Fig. 4. It becomes evident that as more collisions occur, the amount of entanglement generated between the latest pairs of electrons tends to decrease. This is expected since the proton keeps moving farther away with more momentum as more collisions take place and so each consecutive electron carries less relative momentum with respect to the proton. In addition to this, there is a physical restriction at play, namely the monogamy of entanglement [34]. The latter result essentially states that, in order for two qubits A and B to be maximally entangled, they must not be entangled with a third subsystem C. Since all involved particles are entangled in this case, no pair of particles can ever be maximally entangled. In fact, only the

bipartition proton and electrons can actually reach maximal entanglement.

V. CONCLUSIONS

In this work we studied how the consecutive scatterings of particles (originating from the same source) with a central target particle can be used to generate a multipartite entangled state between all particles. In particular, we showed that the amount of bipartite entanglement entanglement between pairs of particles, as quantified by the concurrence, is a balance between two factors. On one hand, the entanglement increases the closer the projectile particle is to total reflection as well as how close its mass is to the target particle's. On the other hand, the entanglement decreases with the number of collisions while at the same time making it harder for consecutive projectile particles to hit the target particle. For the specific case of electrons scattering off a proton, it is clear that any appreciable entanglement is concentrated on a small solid angle centered around the total reflected direction, with larger angular apertures for larger mass ratios. It was also shown that there is always a momentum for which the generated entanglement achieves a maximum value, which can be associated to an optimal point of interaction lying between the extremes of small and large momenta, where the projectile and target particles barely interact.

As a method to generate multipartite quantum states of massive particles, the consecutive scatterings of particles from a heavier target particle is conceptually much simpler than most currently used methods. Nevertheless, there are two clear bottlenecks to be addressed for experimental implementations. First, for small mass ratios (the easiest to implement) one would need to focus on totally reflected particles, whose direction collides with the newly projected particles. Second, the heavier target particle would need to be as static as possible for the projectile particles to hit it, and the method used to keep it still could influence the projected particles in nontrivial ways. While the second difficulty would evidently be harder to address, a solution to the first one might be to use magnetic fields to alter the trajectory of the projectile particles, which would not change their energies. One would need, however, to take into account the inevitable effects of spin precession in the helicity qubit degrees of freedom.

APPENDIX A: EXPLICIT STATE CONSTRUCTION FOR TWO PROJECTILE-TARGET SCATTERINGS

Consider an initial state composed by a target with four-momentum $\mathbf{p}_1$ and helicity h_1 and two projectiles with momenta $\mathbf{p}_2$, $\mathbf{p}_3$ and helicities h_2 and h_3. Consider as

well the unitary matrix defined by

$$\hat{U}_{i,j}|\mathbf{p}_1, r_1; \ldots; \mathbf{p}_n, r_n\rangle \equiv (\hat{U}|\mathbf{p}_i, r_i; \mathbf{p}_j, r_j\rangle) \otimes |\mathbf{p}_1, r_1; \ldots; \mathbf{p}_{i-1}, r_{i-1}; \mathbf{p}_{i+1}, r_{i+1}; \ldots; \mathbf{p}_{j-1}, r_{j-1}; \mathbf{p}_{j+1}, r_{j+1}; \ldots; \mathbf{p}_n, r_n\rangle, \quad \text{(A1)}$$

i.e., it applies the unitary evolution operator $\hat{U}$, defined by Eq. (2), on the two particles indexed by i and j (the positions relative to the initial ket). Using this notation, the scattering of a target particle with one projectile particle, followed by another scattering of the same target with another projectile, will result in a final state of the form

$$|\psi(t_f)\rangle = \hat{U}_{1,3}\hat{U}_{1,2}|\mathbf{p}_1, r_1; \mathbf{p}_2, r_2; \mathbf{p}_3, r_3\rangle. \quad \text{(A2)}$$

To find the explicit form of this state, one may note the specific form of Eq. (6) for two-particle scatterings, namely

$$\hat{U}_{1,2}|\mathbf{p}_1, h_1; \mathbf{p}_2, h_2\rangle = |\mathbf{p}_1, h_1; \mathbf{p}_2, h_2\rangle + i \int \frac{d^3\mathbf{q}_1}{(2\pi)^3 2E_{\mathbf{q}_1}} \frac{d^3\mathbf{q}_2}{(2\pi)^3 2E_{\mathbf{q}_2}} (2\pi)^4 \delta^{(4)}(q_1 + q_2 - p_1 - p_2)$$

$$\times \sum_{r_1, r_3} \mathcal{M}(\mathbf{q}_1, r_1; \mathbf{q}_2, r_2 | \mathbf{p}_1, h_1; \mathbf{p}_2, h_2)|\mathbf{q}_1, r_1; \mathbf{q}_2, r_2\rangle. \quad \text{(A3)}$$

We can now start by considering the first scattering only, whose resulting state is

$$\hat{U}_{1,2}|\mathbf{p}_1, h_1; \mathbf{p}_2, h_2; \mathbf{p}_3, h_3\rangle = |\mathbf{p}_1, h_1; \mathbf{p}_2, h_2; \mathbf{p}_3, h_3\rangle + i \int \frac{d^3\mathbf{q}_1}{(2\pi)^3 2E_{\mathbf{q}_1}} \frac{d^3\mathbf{q}_2}{(2\pi)^3 2E_{\mathbf{q}_2}} (2\pi)^4 \delta^{(4)}(q_1 + q_2 - p_1 - p_2)$$

$$\times \sum_{r_1, r_2} \mathcal{M}(\mathbf{q}_1, r_1; \mathbf{q}_2, r_2 | \mathbf{p}_1, h_1; \mathbf{p}_2, h_2)|\mathbf{q}_1, r_1; \mathbf{q}_2, r_2; \mathbf{p}_3, h_3\rangle. \quad \text{(A4)}$$

The second target-projectile scattering, encoded by $\hat{U}_{1,3}$, results in the state

$$\hat{U}_{1,3}\hat{U}_{1,2}|\mathbf{p}_1, h_1; \mathbf{p}_2, h_2; \mathbf{p}_3, h_3\rangle = \hat{U}_{1,3}|\mathbf{p}_1, h_1; \mathbf{p}_3, h_3\rangle \otimes |\mathbf{p}_2, h_2\rangle + i \int \frac{d^3\mathbf{q}_1}{(2\pi)^3 2E_{\mathbf{q}_1}} \frac{d^3\mathbf{q}_2}{(2\pi)^3 2E_{\mathbf{q}_2}} (2\pi)^4 \delta^{(4)}(q_1 + q_2 - p_1 - p_2)$$

$$\times \sum_{r_1, r_2} \mathcal{M}(\mathbf{q}_1, r_1; \mathbf{q}_2, r_2 | \mathbf{p}_1, h_1; \mathbf{p}_2, h_2)\hat{U}_{1,3}|\mathbf{q}_1, r_1; \mathbf{p}_3, h_3\rangle|\mathbf{q}_2, r_2\rangle$$

$$= |\mathbf{p}_1, h_1; \mathbf{p}_2, h_2; \mathbf{p}_3, h_3\rangle + i \int \frac{d^3\mathbf{q}_1}{(2\pi)^3 2E_{\mathbf{q}_1}} \frac{d^3\mathbf{q}_3}{(2\pi)^3 2E_{\mathbf{q}_3}} (2\pi)^4 \delta^{(4)}(q_1 + q_3 - p_1 - p_3)$$

$$\times \sum_{r_1, r_2} \mathcal{M}(\mathbf{q}_1, r_1; \mathbf{q}_3, r_3 | \mathbf{p}_1, h_1; \mathbf{p}_3, h_3)|\mathbf{q}_1, r_1; \mathbf{p}_2, h_2; \mathbf{q}_3, r_3\rangle$$

$$+ i \int \frac{d^3\mathbf{q}_1}{(2\pi)^3 2E_{\mathbf{q}_1}} \frac{d^3\mathbf{q}_2}{(2\pi)^3 2E_{\mathbf{q}_2}} (2\pi)^4 \delta^{(4)}(q_1 + q_2 - p_1 - p_2) \sum_{r_1, r_2} \mathcal{M}(\mathbf{q}_1, r_1; \mathbf{q}_2, r_2 | \mathbf{p}_1, h_1; \mathbf{p}_2, h_2)$$

$$\times \left(|\mathbf{q}_1, r_1; \mathbf{p}_3, h_3\rangle + i \int \frac{d^3\mathbf{k}_1}{(2\pi)^3 2E_{\mathbf{k}_1}} \frac{d^3\mathbf{k}_3}{(2\pi)^3 2E_{\mathbf{k}_3}} (2\pi)^4 \delta^{(4)}(q_1 + p_3 - k_1 - k_3) \right.$$

$$\left. \times \sum_{l_1, l_3} \mathcal{M}(\mathbf{k}_1, l_1; \mathbf{k}_3, l_3 | \mathbf{q}_1, r_1; \mathbf{p}_3, h_3)|\mathbf{k}_1, l_1; \mathbf{k}_3, l_3\rangle \right)|\mathbf{q}_2, r_2\rangle \quad \text{(A5)}$$

$$= |\mathbf{p}_1, h_1; \mathbf{p}_2, h_2; \mathbf{p}_3, h_3\rangle + i \int \frac{d^3\mathbf{q}_1}{(2\pi)^3 2E_{\mathbf{q}_1}} \frac{d^3\mathbf{q}_3}{(2\pi)^3 2E_{\mathbf{q}_3}} (2\pi)^4 \delta^{(4)}(q_1 + q_3 - p_1 - p_3)$$

$$\times \sum_{r_1, r_2} \mathcal{M}(\mathbf{q}_1, r_1; \mathbf{q}_3, r_3 | \mathbf{p}_1, h_1; \mathbf{p}_3, h_3)|\mathbf{q}_1, r_1; \mathbf{p}_2, h_2; \mathbf{q}_3, r_3\rangle$$

$$+ i \int \frac{d^3\mathbf{q}_1}{(2\pi)^3 2E_{\mathbf{q}_1}} \frac{d^3\mathbf{q}_2}{(2\pi)^3 2E_{\mathbf{q}_2}} (2\pi)^4 \delta^{(4)}(q_1 + q_2 - p_1 - p_2) \sum_{r_1, r_2} \mathcal{M}(\mathbf{q}_1, r_1; \mathbf{q}_2, r_2 | \mathbf{p}_1, h_1; \mathbf{p}_2, h_2)$$

$$\times |\mathbf{q}_1, r_1; \mathbf{q}_2, r_2; \mathbf{p}_3, h_3\rangle + i^2 \int \frac{d^3\mathbf{q}_1}{(2\pi)^3 2E_{\mathbf{q}_1}} \frac{d^3\mathbf{q}_2}{(2\pi)^3 2E_{\mathbf{q}_2}} \frac{d^3\mathbf{k}_1}{(2\pi)^3 2E_{\mathbf{k}_1}} \frac{d^3\mathbf{k}_3}{}$$

$$\times (2\pi)^3 2E_{\mathbf{k}_3}(2\pi)^8 \delta^{(4)}(q_1 + q_2 - p_1 - p_2)\delta^{(4)}(q_1 + p_3 - k_1 - k_3)$$

$$\times \sum_{r_1, r_2, l_1, l_3} \mathcal{M}(\mathbf{k}_1, l_1; \mathbf{k}_3, l_3 | \mathbf{q}_1, r_1; \mathbf{p}_3, h_3)\,\mathcal{M}(\mathbf{q}_1, r_1; \mathbf{q}_2, r_2 | \mathbf{p}_1, h_1; \mathbf{p}_2, h_2)|\mathbf{k}_1, l_1; \mathbf{q}_2, r_2; \mathbf{k}_3, l_3\rangle. \quad \text{(A6)}$$

The final state is thus a superposition of four states: one where no scattering occurred, two others where one of the scatterings did not occur, and a final one where all scatterings happened. Using now the normalization relation

$$\langle \mathbf{k}, r | \mathbf{p}, s \rangle = (2\pi)^3 \delta_{rs} \delta^{(3)}(\mathbf{k} - \mathbf{p}) 2E_{\mathbf{p}} \tag{A7}$$

we can find the probability amplitude of obtaining as final state a target with momentum $\mathbf{p}_4$ and helicity h_4 as well as two projectiles with momenta $\mathbf{p}_5$ and $\mathbf{p}_6$ and helicities h_5 and h_6. This comes out as

$$\langle \mathbf{p}_4, h_4; \mathbf{p}_5, h_5; \mathbf{p}_6, h_6 | \hat{U}_{1,3} \hat{U}_{1,2} | \mathbf{p}_1, h_1; \mathbf{p}_2, h_2; \mathbf{p}_3, h_3 \rangle$$

$$= i^2 \int \frac{d^3 \mathbf{q}_1}{(2\pi)^3 2E_{\mathbf{q}_1}} \frac{d^3 \mathbf{q}_2}{(2\pi)^3 2E_{\mathbf{q}_2}} \frac{d^3 \mathbf{k}_1}{(2\pi)^3 2E_{\mathbf{k}_1}} \frac{d^3 \mathbf{k}_3}{(2\pi)^3 2E_{\mathbf{k}_3}} (2\pi)^8 \delta^{(4)}(q_1 + q_2 - p_1 - p_2) \delta^{(4)}(q_1 + p_3 - k_1 - k_3)$$

$$\times (2\pi)^3 \delta_{h_4 l_1} \delta^{(3)}(\mathbf{k}_1 - \mathbf{p}_4) 2E_{\mathbf{k}_1} (2\pi)^3 \delta_{h_5 r_2} \delta^{(3)}(\mathbf{q}_2 - \mathbf{p}_5) 2E_{\mathbf{q}_2} (2\pi)^3 \delta_{h_6 l_3} \delta^{(3)}(\mathbf{k}_3 - \mathbf{p}_6) 2E_{\mathbf{k}_3}$$

$$\times \sum_{r_1, r_2, l_1, l_3} \mathcal{M}(\mathbf{k}_1, l_1; \mathbf{k}_3, l_3 | \mathbf{q}_1, r_1; \mathbf{p}_3, h_3) \mathcal{M}(\mathbf{q}_1, r_1; \mathbf{q}_2, r_2 | \mathbf{p}_1, h_1; \mathbf{p}_2, h_2)$$

$$= - \int \frac{d^3 \mathbf{q}_1}{2E_{\mathbf{q}_1}} (2\pi)^5 \delta^{(4)}(q_1 + p_5 - p_1 - p_2) \delta^{(4)}(q_1 + p_3 - p_4 - p_6)$$

$$\times \sum_{r_1} \mathcal{M}(\mathbf{p}_4, h_4; \mathbf{p}_6, h_6 | \mathbf{q}_1, r_1; \mathbf{p}_3, h_3) \mathcal{M}(\mathbf{q}_1, r_1; \mathbf{p}_5, h_5 | \mathbf{p}_1, h_1; \mathbf{p}_2, h_2)$$

$$= - \frac{(2\pi)^5}{2E_{\mathbf{p}_5 - \mathbf{p}_1 - \mathbf{p}_2}} \delta(E_{\mathbf{p}_5 - \mathbf{p}_1 - \mathbf{p}_2} + E_{\mathbf{p}_5} - E_{\mathbf{p}_1} - E_{\mathbf{p}_2}) \delta(E_{\mathbf{p}_5 - \mathbf{p}_1 - \mathbf{p}_2} + E_{\mathbf{p}_3} - E_{\mathbf{p}_4} - E_{\mathbf{p}_6}) \delta^{(3)}(\mathbf{p}_1 + \mathbf{p}_2 + \mathbf{p}_3 - \mathbf{p}_5 - \mathbf{p}_4 - \mathbf{p}_6)$$

$$\times \sum_{r_1} \mathcal{M}(\mathbf{p}_4, h_4; \mathbf{p}_6, h_6 | \mathbf{p}_5 - \mathbf{p}_1 - \mathbf{p}_2, r_1; \mathbf{p}_3, h_3) \mathcal{M}(\mathbf{p}_5 - \mathbf{p}_1 - \mathbf{p}_2, r_1; \mathbf{p}_5, h_5 | \mathbf{p}_1, h_1; \mathbf{p}_2, h_2)$$

$$\equiv \mathcal{N}_3 d_{h_4 h_5 h_6}(\mathbf{p}_4, \mathbf{p}_5, \mathbf{p}_6), \tag{A8}$$

where

$$d_{h_4 h_5 h_6}(\mathbf{p}_4, \mathbf{p}_5, \mathbf{p}_6) = \sum_{r_1} \mathcal{M}(\mathbf{p}_4, h_4; \mathbf{p}_6, h_6 | \mathbf{p}_5 - \mathbf{p}_1 - \mathbf{p}_2, r_1; \mathbf{p}_3, h_3) \mathcal{M}(\mathbf{p}_5 - \mathbf{p}_1 - \mathbf{p}_2, r_1; \mathbf{p}_5, h_5 | \mathbf{p}_1, h_1; \mathbf{p}_2, h_2) \tag{A9}$$

and we formally take

$$\mathcal{N}_3 = - \frac{(2\pi)^5}{2E_{\mathbf{p}_5 - \mathbf{p}_1 - \mathbf{p}_2}} \delta(E_{\mathbf{p}_5 - \mathbf{p}_1 - \mathbf{p}_2} + E_{\mathbf{p}_5} - E_{\mathbf{p}_1} - E_{\mathbf{p}_2}) \delta(E_{\mathbf{p}_5 - \mathbf{p}_1 - \mathbf{p}_2} + E_{\mathbf{p}_3} - E_{\mathbf{p}_4} - E_{\mathbf{p}_6}) \tag{A10}$$

to be a constant. One sees that $\mathcal{N}_3$ naturally contains conservation of energy and momentum over the set of scatterings that occur.

We are now interested in analyzing the entanglement created in the helicity degrees of freedom of the final outgoing state in the case where the two scatterings occur. This amounts to looking at the helicity component of the final state, which will have the form

$$|\psi_h\rangle = \mathcal{N}_3 \sum_{h_4, h_5, h_6} d_{h_4 h_5 h_6}(\mathbf{p}_4, \mathbf{p}_5, \mathbf{p}_6) |h_4, h_5, h_6\rangle. \tag{A11}$$

One may now trace away the target subsystem and check if the remaining parts, composed by the two projectiles, are entangled. In order to do that, one must first build the density matrix. Noting that $\mathcal{N}_3$ only involves real quantities, we may consider that $\mathrm{Tr}[|\psi_h\rangle \langle \psi_h|] = \mathcal{N}^2 \sum_{h_4, h_5, h_6} |d_{h_4 h_5 h_6}(\mathbf{p}_4, \mathbf{p}_5, \mathbf{p}_6)|^2$, so that a normalized density matrix for the final state is

$$\rho_{t,p,p} = \frac{|\psi_h\rangle \langle \psi_h|}{\mathrm{Tr}[|\psi_h\rangle \langle \psi_h|]} = \frac{\sum_{h_4, h_5, h_6, r_4, r_5, r_6} d_{h_4 h_5 h_6}(\mathbf{p}_4, \mathbf{p}_5, \mathbf{p}_6) d^*_{r_4 r_5 r_6}(\mathbf{p}_4, \mathbf{p}_5, \mathbf{p}_6) |h_4, h_5, h_6\rangle \langle r_4, r_5, r_6|}{\sum_{h_4, h_5, h_6} |d_{h_4 h_5 h_6}(\mathbf{p}_4, \mathbf{p}_5, \mathbf{p}_6)|^2}, \tag{A12}$$

where we used the indexes t and p to refer to target and projectile subsystems, respectively. Note that the factor of $\mathcal{N}_3$ has formally been canceled out. Tracing out the target subsystem results in the system composed by the two projectiles, whose entanglement properties we can then investigate.

We must now perform the partial trace of the helicity qubits related to the proton, which amounts to applying the formula

$$\mathrm{Tr}_t[\rho] = \sum_{\sigma} (I_r \otimes \langle \sigma |_t) \rho (I_r \otimes |\sigma\rangle_t), \tag{A13}$$

where I_r represents the identity acting on the remaining subsystems. Defining for simplicity

$$\mathcal{N}_\rho = \sum_{h_4, h_5, h_6} |d_{h_4 h_5 h_6}(\mathbf{p}_4, \mathbf{p}_5, \mathbf{p}_6)|^2 \tag{A14}$$

we obtain the partially traced density matrix

$$\rho_{p,p} = \mathrm{Tr}_t[\rho_{t,p,p}] = \mathcal{N}_\rho^{-1} \sum_{\sigma, h_4, h_5, h_6, r_4, r_5, r_6} d_{h_4 h_5 h_6}(\mathbf{p}_4, \mathbf{p}_5, \mathbf{p}_6) d_{r_4 r_5 r_6}^*(\mathbf{p}_4, \mathbf{p}_5, \mathbf{p}_6)|h_5, h_6\rangle \langle r_5, r_6|$$

$$= \sum_{h_5, h_6, r_5, r_6} \rho_{h_5 h_6 r_5 r_6} |h_5, h_6\rangle \langle r_5, r_6|, \tag{A15}$$

where we have the reduced density matrix components

$$\rho_{h_5 h_6 r_5 r_6} = \mathcal{N}_\rho^{-1} \left(\sum_\sigma d_{\sigma h_5 h_6}(\mathbf{p}_4, \mathbf{p}_5, \mathbf{p}_6) d_{\sigma r_5 r_6}^*(\mathbf{p}_4, \mathbf{p}_5, \mathbf{p}_6) \right). \tag{A16}$$

The matrix $\rho_{p,p}$ has trace equal to 1, as can be straightforwardly checked and will in general be mixed, i.e., $\mathrm{Tr}[\rho_{e,e}^2] < 1$.

APPENDIX B: KINEMATICS FOR CONSECUTIVE COLLISIONS

Here we demonstrate the steps required to reproduce in all generality the kinematics for the consecutive collisions that take place in the main body of the paper. For the sake of generalization, we will employ a different notation for the ingoing and outgoing momenta, as depicted in Fig. 5.

Let $\mathbf{p}_{\mathrm{in}}^{(1)}$ be the three-momentum of the target particle, which starts of at rest and has mass M. The superscript "(1)" indicate that we are referring to the first scattering that particle $\mathbf{p}$ is experiencing, while the subscript "in" indicates that it is an incoming particle. The other incoming particle in the first scattering will be denoted by $\mathbf{k}_{\mathrm{in}}^{(1)}$, which is the particle that will be accelerated towards the target particle with linear momentum p and mass m. After a single scattering, the outgoing three-momenta are $\mathbf{p}_{\mathrm{out}}^{(1)}$ and $\mathbf{k}_{\mathrm{out}}^{(1)}$. From here, we want to consider additional copies of the particle $\mathbf{k}_{\mathrm{in}}^{(1)}$ to consecutively scatter against the same target particle, so for the second
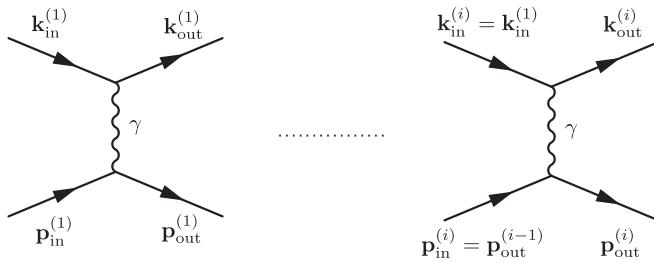

FIG. 5. Diagram depicting the consecutive scatterings. The diagrams represent the tree-level QED interaction between two distinguishable types of particles denoted by the three-momenta $\mathbf{k}$ and $\mathbf{p}$, with rest masses m and M, respectively. The superscripts in the three-momenta indicate how many interactions occurred up to that point, while the subscripts indicate whether the particle is incoming or outgoing. The three-momenta $\mathbf{p}$ indicate the target particle, which started off at rest, while $\mathbf{k}$ is the lighter particle, which is accelerated into the target. For each interaction, a different particle $\mathbf{k}$, with the same energy and direction as the first one, is shot at the same target particle $\mathbf{p}$, such that the in the ith interaction, $\mathbf{k}_{\mathrm{in}}^{(i)} = \mathbf{k}_{\mathrm{in}}^{(1)}$, while $\mathbf{p}_{\mathrm{in}}^{(i)} = \mathbf{p}_{\mathrm{out}}^{(i-1)}$.

collision we will have $\mathbf{k}_{\mathrm{in}}^{(2)} = \mathbf{k}_{\mathrm{in}}^{(1)}$ scattering off of $\mathbf{p}_{\mathrm{in}}^{(2)} = \mathbf{p}_{\mathrm{out}}^{(1)}$, and so on for any number of intended collisions. With this we set up the first conditions for our system of consecutive collisions, which will allow us to recursively compute the kinematics in the ith interaction. In particular, we have:

$$\mathbf{p}_{\mathrm{in}}^{(1)} = (0, 0, 0), \tag{B1}$$

$$\mathbf{k}_{\mathrm{in}}^{(1)} = (0, 0, p), \tag{B2}$$

$$\mathbf{p}_{\mathrm{in}}^{(i)} = \mathbf{p}_{\mathrm{out}}^{(i-1)}, \tag{B3}$$

$$\mathbf{k}_{\mathrm{in}}^{(i)} = \mathbf{k}_{\mathrm{in}}^{(1)}. \tag{B4}$$

As we will see, each interaction will result in an additional two degrees of freedom, which we will take as the angular coordinates for the outgoing particle $\mathbf{k}_{\mathrm{out}}^{(i)}$, namely $\theta_{\mathbf{k}}^{(i)}$ and $\phi_{\mathbf{k}}^{(i)}$. Due to spherical symmetry, one can eliminate a single degree of freedom $\phi_{\mathbf{k}}^{(i)}$, which we choose to be $\phi_{\mathbf{k}}^{(1)}$ in this work, although any other $\phi_{\mathbf{k}}^{(i)}$ is possible. In order to find the values of $\mathbf{p}_{\mathrm{out}}^{(i)}$ and $\mathbf{k}_{\mathrm{out}}^{(i)}$ as functions of $\theta_{\mathbf{k}}^{(i)}$ and $\phi_{\mathbf{k}}^{(i)}$, we only need to guarantee that these can be recursively calculated from $\mathbf{p}_{\mathrm{out}}^{(i-1)} = \mathbf{p}_{\mathrm{in}}^{(i)}$.

Let $E_{\mathbf{k}}$ and $E_{\mathbf{p}}$ denote the energies the particles with momenta $\mathbf{k}$ and $\mathbf{p}$, respectively. From the conservation of four-momentum leading to the equality $(k_{\mathrm{in}}^{(i)} - k_{\mathrm{out}}^{(i)})^2 = (p_{\mathrm{out}}^{(i)} - p_{\mathrm{in}}^{(i)})^2$ and from the conservation of energy $E_{\mathbf{p}_{\mathrm{out}}^{(i)}} = E_{\mathbf{k}_{\mathrm{in}}^{(i)}} + E_{\mathbf{p}_{\mathrm{in}}^{(i)}} - E_{\mathbf{k}_{\mathrm{out}}^{(i)}}$, one can write

$$\sqrt{\left|\mathbf{k}_{\mathrm{out}}^{(i)}\right|^2 + m^2} = a + b\left|\mathbf{k}_{\mathrm{out}}^{(i)}\right|, \tag{B5}$$

with

$$a \equiv E_{\mathbf{p}_{\mathrm{in}}^{(i)}} - \frac{M^2 - m^2 + \mathbf{p}_{\mathrm{in}}^{(i)} \cdot \left(\mathbf{p}_{\mathrm{in}}^{(i)} + \mathbf{k}_{\mathrm{in}}^{(i)}\right)}{E_{\mathbf{k}_{\mathrm{in}}^{(i)}} + E_{\mathbf{p}_{\mathrm{in}}^{(i)}}}, \tag{B6}$$

$$b \equiv \frac{\vec{e}(\theta_{\mathbf{k}}^{(i)}, \phi_{\mathbf{k}}^{(i)}) \cdot \left(\mathbf{p}_{\mathrm{in}}^{(i)} + \mathbf{k}_{\mathrm{in}}^{(i)}\right)}{E_{\mathbf{k}_{\mathrm{in}}^{(i)}} + E_{\mathbf{p}_{\mathrm{in}}^{(i)}}}, \tag{B7}$$

where $\vec{e}(\theta_{\mathbf{k}}^{(i)}, \phi_{\mathbf{k}}^{(i)})$ is the unit vector for $\mathbf{k}_{\text{out}}^{(i)} = |\mathbf{k}_{\text{out}}^{(i)}|\vec{e}(\theta_{\mathbf{k}}^{(i)}, \phi_{\mathbf{k}}^{(i)})$. Equation (B5) is solvable for $|\mathbf{k}_{\text{out}}^{(i)}|$ with a single positive solution

$$\left|\mathbf{k}_{\text{out}}^{(i)}\right| = \frac{a\,b + \sqrt{a^2 + m^2(b^2 - 1)}}{b^2 - 1}, \tag{B8}$$

and, so long as we know $\mathbf{p}_{\text{in}}^{(i)} = \mathbf{p}_{\text{out}}^{(i-1)}$, we can explicitly write Eq. (B8), which itself is enough to fully describe $\mathbf{k}_{\text{out}}^{(i)}$ as well as $\mathbf{p}_{\text{out}}^{(i)}$ (through three-momentum conservation).

Finally, when calculating the scattering amplitudes it can be useful to define the angular coordinates $(\theta_{\mathbf{p}}^{(i)}, \phi_{\mathbf{p}}^{(i)})$ associated to the direction of $\mathbf{p}_{\text{out}}^{(i)}$, to be used for the spinors in the helicity basis. These are straightforward to derive from $\mathbf{p}_{\text{out}}^{(i)}$. Let us consider the first interaction as an example. This case is simpler since $\mathbf{p}_{\text{in}}^{(1)} = (0, 0, 0)$, as well as by the fact that we can fix $\phi_{\mathbf{k}}^{(1)} = 0$ from spherical symmetry. As such, Eq. (B8) reads

$$\left|\mathbf{k}_{\text{out}}^{(1)}\right| = p \frac{(m^2 + M\sqrt{p^2 + m^2})\cos\left(\theta_{\mathbf{k}}^{(1)}\right) + (M + \sqrt{p^2 + m^2})\sqrt{M^2 - m^2 \sin^2\left(\theta_{\mathbf{k}}^{(1)}\right)}}{(M + \sqrt{p^2 + m^2})^2 - p^2 \cos^2\left(\theta_{\mathbf{k}}^{(1)}\right)}. \tag{B9}$$

The form of $\mathbf{k}_{\text{out}}^{(1)}$ leads to a solution for $\mathbf{p}_{\text{out}}^{(1)}$, which in turn leads to a recursive solution for any ith interaction as given by Eqs. (B1)–(B4).

---

[1] S. Popescu, Bell's inequalities and density matrices: Revealing hidden nonlocality, Phys. Rev. Lett. **74**, 2619 (1995).

[2] C. H. Bennett, G. Brassard, S. Popescu, B. Schumacher, J. A. Smolin, and W. K. Wootters, Purification of noisy entanglement and faithful teleportation via noisy channels, Phys. Rev. Lett. **76**, 722 (1996).

[3] C. H. Bennett, D. P. DiVincenzo, J. A. Smolin, and W. K. Wootters, Mixed-state entanglement and quantum error correction, Phys. Rev. A **54**, 3824 (1996).

[4] J. M. Raimond, M. Brune, and S. Haroche, Manipulating quantum entanglement with atoms and photons in a cavity, Rev. Mod. Phys. **73**, 565 (2001).

[5] A. Beige, S. Bose, D. Braun, S. F. Huelga, P. L. Knight, M. B. Plenio, and V. Vedral, Entangling atoms and ions in dissipative environments, J. Mod. Opt. **47**, 2583 (2000).

[6] J. I. Cirac and P. Zoller, New frontiers in quantum information with atoms and ions, Phys. Today **57**(3), 38 (2004).

[7] A. Mandilara, V. M. Akulin, M. Kolar, and G. Kurizki, Control of multiatom entanglement in a cavity, Phys. Rev. A **75**, 022327 (2007).

[8] J. F. Traub, Introduction to Quantum information science, in *Encyclopedia of Complexity and Systems Science*, edited by R. A. Meyers (Springer, New York, 2009), pp. 7399–7400.

[9] R. Laflamme, C. Miquel, J. P. Paz, and W. H. Zurek, Perfect quantum error correcting code, Phys. Rev. Lett. **77**, 198 (1996).

[10] M. A. Nielsen and I. L. Chuang, *Quantum Computation and Quantum Information: 10th Anniversary Edition* (Cambridge University Press, Cambridge, 2010).

[11] R. Jozsa and N. Linden, On the role of entanglement in quantum computational speed-up, Proc. R. Soc. Lond. A **459**, 2011 (2003).

[12] M. Blasone, F. Dell'Anno, S. D. Siena, and F. Illuminati, Entanglement in neutrino oscillations, Europhys. Lett. **85**, 50002 (2009).

[13] B. Kayser, J. Kopp, R. G. H. Robertson, and P. Vogel, Theory of neutrino oscillations with entanglement, Phys. Rev. D **82**, 093003 (2010).

[14] M. Blasone, F. Dell'Anno, S. De Siena, and F. Illuminati, Neutrino flavor entanglement, Proceedings of the Neutrino Oscillation Workshop, Nucl. Phys. B Proceedings Supplements **320**, 237 (2013).

[15] M. Blasone, F. Dell'Anno, S. D. Siena, and F. Illuminati, A field-theoretical approach to entanglement in neutrino mixing and oscillations, Europhys. Lett. **106**, 30002 (2014).

[16] G. M. Quinta, A. Sousa, and Y. Omar, Predicting leptonic CP violation via minimization of neutrino entanglement, arXiv:2207.03303 [hep-ph].

[17] A. Cervera-Lierta, J. I. Latorre, J. Rojo, and L. Rottoli, Maximal entanglement in high energy physics, SciPost Phys. **3**, 036 (2017).

[18] S. Fedida and A. Serafini, Tree-level entanglement in quantum electrodynamics, Phys. Rev. D **107**, 116007 (2023).

[19] J. B. Araujo, B. Hiller, I. G. da Paz, M. M. Ferreira, Jr., M. Sampaio, and H. A. S. Costa, Measuring QED cross sections via entanglement, Phys. Rev. D **100**, 105018 (2019).

[20] Y. Afik and J. R. M. d. Nova, Quantum information with top quarks in QCD, Quantum **6**, 820 (2022).

[21] R. Peschanski and S. Seki, Entanglement entropy of scattering particles, Phys. Lett. B **758**, 89 (2016).

[22] A. Bose, P. Haldar, A. Sinha, P. Sinha, and S. S. Tiwari, Relative entropy in scattering and the S-matrix bootstrap, SciPost Phys. **9**, 081 (2020).

[23] A. Sinha and A. Zahed, Bell inequalities in 2-2 scattering, Phys. Rev. D **108**, 025015 (2023).

[24] G. A. Miller, Entanglement of elastic and inelastic scattering, Phys. Rev. C **108**, L041601 (2023).

[25] G. A. Miller, Entanglement maximization in low-energy neutron-proton scattering, Phys. Rev. C **108**, L031002 (2023).

[26] T. Kirchner, W. Elkamhawy, and H.-W. Hammer, Entanglement in few-nucleon scattering events, arXiv:2312.14484 [nucl-th].

[27] R. A. Morales, Exploring Bell inequalities and quantum entanglement in vector boson scattering, arXiv:2306.17247 [hep-ph].

[28] S. R. Beane, D. B. Kaplan, N. Klco, and M. J. Savage, Entanglement suppression and emergent symmetries of strong interactions, Phys. Rev. Lett. **122**, 102001 (2019).

[29] I. Low and T. Mehen, Symmetry from entanglement suppression, Phys. Rev. D **104**, 074014 (2021).

[30] Q. Liu, I. Low, and T. Mehen, Minimal entanglement and emergent symmetries in low-energy QCD, Phys. Rev. C **107**, 025204 (2023).

[31] S. R. Beane, R. C. Farrell, and M. Varma, Entanglement minimization in hadronic scattering with pions, Int. J. Mod. Phys. A **36**, 2150205 (2021).

[32] M. Carena, I. Low, C. E. M. Wagner, and M.-L. Xiao, Entanglement Suppression, Enhanced symmetry and a standard-model-like Higgs boson, arXiv:2307.08112 [hep-ph].

[33] M. E. Peskin and D. V. Schroeder, *An Introduction to Quantum Field Theory* (Addison-Wesley, Reading, 1995).

[34] V. Coffman, J. Kundu, and W. K. Wootters, Distributed entanglement, Phys. Rev. A **61**, 052306 (2000).